Neuropharmacology 98 (2015) 68–77

Contents lists available at ScienceDirect

Neuropharmacology

journal homepage: www.elsevier.com/locate/neuropharm

# Direct visualisation of internalization of the adenosine $A_3$ receptor and localization with arrestin3 using a fluorescent agonist

Leigh A. Stoddart [a], Andrea J. Vernall [b], Stephen J. Briddon [a], Barrie Kellam [b], Stephen J. Hill [a, *]

[a] Cell Signalling Research Group, School of Life Sciences, Queen's Medical Centre, University of Nottingham, NG7 2UH, UK
[b] School of Pharmacy, Centre for Biomolecular Sciences, University of Nottingham, University Park, Nottingham, NG7 2RD, UK

ARTICLE INFO

*Article history:*
Available online 30 April 2015

*Keywords:*
Adenosine receptors
Adenosine $A_3$ receptor
Fluorescent agonist
Internalization
Arrestin3

ABSTRACT

Fluorescence based probes provide a novel way to study the dynamic internalization process of G protein-coupled receptors (GPCRs). Recent advances in the rational design of fluorescent ligands for GPCRs have been used here to generate new fluorescent agonists containing tripeptide linkers for the adenosine $A_3$ receptor. The fluorescent agonist BY630-X-(*D*)-A-(*D*)-A-G-ABEA was found to be a highly potent agonist at the adenosine $A_3$ receptor in both reporter gene ($pEC_{50} = 8.48 \pm 0.09$) and internalization assays ($pEC_{50} = 7.47 \pm 0.11$). Confocal imaging studies showed that BY630-X-(*D*)-A-(*D*)-A-G-ABEA was internalized with $A_3$ linked to yellow fluorescent protein, which was blocked by the competitive antagonist MRS1220. Internalization of untagged adenosine $A_3$ could also be visualized with BY630-X-(*D*)-A-(*D*)-A-G-ABEA treatment. Further, BY630-X-(*D*)-A-(*D*)-A-G-ABEA stimulated the formation of receptor–arrestin3 complexes and was found to localize with these intracellular complexes. This highly potent agonist with excellent imaging properties should be a valuable tool to study receptor internalization.

This article is part of the Special Issue entitled 'Fluorescent Tools in Neuropharmacology'.



## 1. Introduction

The nucleoside adenosine exerts its biological function via four cell surface G protein-coupled receptors (GPCRs); $A_1$, $A_{2A}$, $A_{2B}$ and $A_3$ (Fredholm et al., 2001; Hill et al., 2014). These receptors have been implicated in a wide range of biological processes, including regulation of the sleep–wake cycle (Huang et al., 2007), regulation of immune cell function (Ohta and Sitkovsky, 2001), locomotion (Yang et al., 2009) and response to hypoxia (Wan et al., 2008). In turn, the dysregulation of these processes can lead to a range of different pathological states such as Parkinson's (Jenner et al., 2009) and Alzheimer's (Chen et al., 2007) diseases, autoimmune disorders (Ohta and Sitkovsky, 2001) and tissue damage following reperfusion injury (Wan et al., 2008). These receptors therefore represent attractive drug targets (Chen et al., 2013).

A greater understanding of the precise downstream signal induced by an agonist, and the subsequent regulation of GPCR function, may allow development of more effective drugs. The adenosine receptors signal through different G proteins, with the $A_1$ and $A_3$ receptors ($A_1$R and $A_3$R) predominately coupling to $G_{i/o}$ and $A_{2A}$ and $A_{2B}$ receptors ($A_{2A}$R and $A_{2B}$R) coupling to $G_s$. It has also been shown that different agonists can activate different downstream signalling cascades (Verzijl and Ijzerman, 2011). Understanding this signalling bias may allow compounds to be developed that target one signalling pathway over another (Kenakin, 2012). The four adenosine receptors show marked differences in their regulation in response to agonist treatment. The $A_{2A}$R, $A_{2B}$R and $A_3$R receptors have all been shown to desensitize rapidly upon agonist treatment, with $A_3$R desensitization the most rapid (Palmer et al., 1994; Peters et al., 1998; Trincavelli et al., 2000). $A_{2A}$R, $A_{2B}$R and $A_3$R are phosphorylated by G protein-receptor kinases (GRKs) which lead to the recruitment of arrestins and subsequent sequestration from the plasma membrane (Ferguson et al., 2000; Mundell et al., 1998, 2000). In contrast, the $A_1$R desensitizes much more slowly and although the agonist stimulated receptor shows enhanced affinity for GRKs it is unclear if phosphorylation actually occurs (Nie et al., 1997; Ramkumar et al., 1991). It has long been thought that internalization of a receptor leads to termination

* Corresponding author. Tel.: +44 (0)115 823 0082.
*E-mail address:* stephen.hill@nottingham.ac.uk (S.J. Hill).

http://dx.doi.org/10.1016/j.neuropharm.2015.04.013

of the agonist-induced signalling but recent studies have challenged this view. It has been shown that some receptors can continue to signal to the cAMP pathway even after sequestration from the plasma membrane (Boutin et al., 2012; Mullershausen et al., 2009; Werthmann et al., 2012). One way to understand the internalization of a GPCR and the termination of the signal is through the use of fluorescent ligands.

Fluorescent ligands for GPCRs (Vernall et al., 2014) have become increasingly used for studying various aspects of receptor pharmacology (Hill et al., 2014; Stoddart et al., 2013). These ligands allow the visualization of dynamic processes such as receptor internalization, trafficking and diffusion characteristics in the cell membrane (Stoddart et al., 2015, in this issue). Many different fluorescent ligands for the adenosine receptors have been developed that retain both affinity for the receptor and their agonist or antagonist properties (Kozma et al., 2013b). Although the fluorescent agonist-based probes that have been previously developed retained potency and efficacy, their imaging characteristics, such as the need for wash steps and the level of non-specific binding, limit their applications in longer-term dynamic studies. It has been shown for the $A_{2A}R$ and the $A_3R$ that fluorescent agonists can induce clustering of the receptor within the cell but the fluorescent ligands used in these studies needed to be removed from the cells prior to visualization (Brand et al., 2008; Kozma et al., 2013a). To allow the dynamic process of receptor internalization to be fully studied, a fluorescent agonist that does not need to be removed is advantageous as this allows the co-localization of the receptor–ligand complex with various proteins involved in the internalization process to be studied. The choice of fluorophore used to label the agonist can influence the ability of the compound to be visualized in the continued presence of unbound ligand. A red-emitting BODIPY fluorophore is an ideal candidate for use in fluorescent ligands as it is brighter in non-aqueous environments, such as the plasma membrane and therefore specific cell surface fluorescence can be more easily visualized (Baker et al., 2010; May et al., 2010; May et al., 2011).

The present study aimed to improve the imaging properties of the existing adenosine receptor agonist ABEA-X-BY630 (Middleton et al., 2007) to allow its use in long-term imaging studies through the incorporation of a peptide linker; an approach previously shown to improve the affinity, subtype selectivity and also reduce non-specific membrane binding of fluorescent adenosine receptor antagonists (Vernall et al., 2013). The newly synthesized fluorescent agonists developed in this study were functionally characterised at each of the adenosine receptors, as well as for agonist-induced internalization at the $A_1R$ and $A_3R$, and arrestin3 recruitment at the $A_3R$. The data indicated improved properties for monitoring receptor internalization of untagged adenosine receptors.

## 2. Experimental details

### 2.1. Materials

G418, Lipofectamine and Optimem were obtained from Life Technologies (Paisley, UK), foetal calf serum (FCS) from PAA Laboratories (Wokingham, UK) and L-glutamine from Lonza (Basel, Switzerland). NECA [5-(N-ethylcarboxamido)adenosine] and MRS1220 [*N*-[9-Chloro-2-(2-furanyl)[1,2,4]-triazolo[1,5-*c*]quinazolin-5-yl] benzene acetamide] were purchased from Tocris Bioscience (Bristol, UK). 6-(((4,4-Difluoro-5-(2-thienyl)-4-bora-3a,4a-diaza-s-indacene-3-yl)styryloxy)acetyl) aminohexanoic acid, succinimidyl ester (BY630-X-SE) was purchased from Molecular Probes® (Invitrogen, UK). All other chemicals and reagents were obtained from Sigma–Aldrich (Gillingham, UK).

### 2.2. Synthesis of fluorescent ligands

Detailed experimental procedures and compound characterisation are provided in the Supplementary data. In brief, the ABEA pharmacophore and the tripeptides were synthesized independently. The ABEA pharmacophore and the required tripeptide were then coupled in solution-phase, the *N*-terminal peptide protecting group removed to afford a primary amine and this then coupled to the commercially available BY630-X-SE. Fluorescent compounds were purified using semi-preparative high-performance liquid chromatography and purities of all compounds were determined as being ≥95%.

### 2.3. Cell culture

Chinese hamster ovary (CHO) cells stably expressing a cAMP response element-secreted placental alkaline phosphatase (CRE-SPAP) reporter gene expressing the human $A_3R$ (Vernall et al., 2012) or human $A_1R$ (Baker and Hill, 2007) were produced as previously described. For $A_{2A}R$ and $A_{2B}R$ cells lines, CHO CRE-SPAP cells were transfected with cDNA encoding the human $A_{2A}R$ or $A_{2B}R$ (Missouri S&T cDNA Resource Center, MO, USA) using Lipofectamine (Life Technologies, Paisley, UK) according to the manufacturer's instructions. Transfected cells were subjected to selective pressure for 2–3 weeks through the addition of 1 mg/mL$^{-1}$ G418 to the normal growth medium. After this time, the cells were dilution-cloned to obtain cell lines originating from a single cell. To confirm the presence of the receptor, cells were screened for their response to NECA in the CRE-SPAP gene transcription assay. CHO cells expressing $A_3$-YFP (Stoddart et al., 2014) and co-expressing $A_3$-vYc and arrestin3-vYnL (Stoddart et al., 2014) were generated as described previously. The CHO $A_1$-GFP cell line was a gift from Prof. Nigel Birdsall, National Institute for Medical Research, London, UK. All cell lines were maintained in Dulbecco's Modified Eagle Medium:Nutrient Mixture F-12 (DMEM/F12) medium containing 10% FCS and 2 mM L-glutamine at 37 °C in humidified atmosphere of air/$CO_2$ (19:1).

### 2.4. CRE-SPAP gene transcription assay

CRE-SPAP cells expressing one of the four adenosine receptors ($A_1R$, $A_3R$, $A_{2A}R$ or $A_{2B}R$) were grown to confluence in clear 96-well plates. On the day prior to analysis, normal growth medium was removed and replaced with serum-free medium (SFM; DMEM/F12 supplemented with 2 mM L-glutamine). On the day of the experiment, fresh SFM was added to the cells with increasing concentrations of the required test compounds. For the $A_1R$ and $A_3Rs$, cells were incubated with the test compounds (30 min, 37 °C/5% $CO_2$) before the addition of 1 μM forskolin (FSK) for $A_3R$ expressing cells and 3 μM FSK for $A_1R$ cells. No FSK was added to $A_{2A}R$ or $A_{2B}R$ cells. All cells were then incubated for 5 h at 37 °C/5% $CO_2$. After the 5 h incubation, all medium was removed from the cells and replaced with 40 μL of SFM and incubated for a further 1 h. The plates were then incubated at 65 °C for 30 min to destroy the endogenous alkaline phosphatases. After cooling the plates to room temperature, 5 mM 4-nitrophenyl phosphate in a diethanolamine-containing buffer (10% (v/v) diethanolamine, 280 mM NaCl, 500 μM $MgCl_2$, pH 9.85) was added to each well. Plates were incubated for varying times depending on the cell line ($A_1R$, 20 min/37 °C; $A_{2A}R$, 10 min/37 °C; $A_{2B}R$, overnight/room temperature; $A_3R$, 20 min/37 °C) and then the absorbance at 405 nm was measured using a Dynex MRX plate reader (Chelmsford, MA, USA).

### 2.5. Automated imaging of receptor internalization

$A_1$-GFP or $A_3$-YFP expressing cells were grown to confluency in 96-well clear-bottomed, black-walled 96-well plates (μclear base, Greiner Bio One, Stonehouse, UK). On the day of the experiment, normal growth medium was removed and fresh SFM added to the cells containing increasing concentrations of NECA or BY630-X-(*D*)-A-(*D*)-A-G-ABEA and incubated for 1 h at 37 °C/5% $CO_2$. After 1 h, medium and compounds were removed and cells were washed once in phosphate buffer saline (PBS). Cells were then treated with 3% paraformaldehyde solution in PBS for 20 min at room temperature to fix the cells and then washed twice in PBS. The cell nuclei were stained by the addition of the cell permeable dye H33342 (2 μg mL$^{-1}$ in PBS) for 20 min at room temperature, followed by two final washes in PBS. The images were obtained on an ImageXpress Ultra confocal plate reader (Molecular Devices, Sunnyvale, CA, USA). Four central images were obtained per well using a Plan Fluor 40× NA0.6 extra-long working distance objective. GFP and YFP images were obtained by excitation of the fluorescent protein with a 488 nm laser with emission collected through a 525–550 nm band pass filter and H33342 images by excitation with a 405 nm laser line and emission collected through a 447–460 nm band pass filter. The resulting images were subjected to analysis for granules and nuclei using an algorithm within MetaXpress software (Molecular Devices) to generate a granule count per cell for each image (Kilpatrick et al., 2010). Granules were identified as having a diameter of between 7 and 15 μm and nuclei as between 6 and 9 μm and the intensity above background was set for each individual experiment.

### 2.6. Confocal imaging

$A_3$-YFP, $A_3R$ or $A_3$-vYc/arrestin3-vYnL cells were grown to approximately 80% confluency on 8-well Labtek chambered coverglasses (Nunc Nalgene). Cells were washed twice in HEPES-buffered saline solution (HBSS; 25 mM HEPES, 10 mM glucose, 146 mM NaCl, 5 mM KCl, 1 mM $MgSO_4$, 2 mM sodium pyruvate, 1.3 mM $CaCl_2$, 1 mM $NaHCO_3$, pH 7.4) and then fresh HBSS added for analysis. To prevent fluorescent ligand binding, cells were incubated with 1 μM MRS1220 for 30 min prior to the addition of BY630-X-(*D*)-A-(*D*)-A-G-ABEA. Images were obtained after 5 min and 60 min incubation with BY630-X-(*D*)-A-(*D*)-A-G-ABEA at 37 °C. All imaging was performed using a Zeiss LSM710 confocal microscope (Carl Zeiss GmbH,

Jena, Germany) fitted with a 63x plan-Apochromat NA1.4 Ph3 oil-immersion objective. For YFP and reconstituted vYFP (BiFC) 488 nm argon laser was used to excite the fluorophore and the emission was detected using a BP505-530 filter. BY630-X-(*D*)-A-(*D*)-A-G-ABEA was excited using a 633 nm HeNe laser and emission collected through a LP650 filter. Within each experiment, a pinhole diameter of 1 Airy unit was used and the laser power, gain and offset kept constant for each experimental set.

### 2.7. Data analysis

All data were fitted using non-linear regression models within Prism 5 (GraphPad Software, San Diego, CA, USA). $A_{2A}$R, $A_{2B}$R and $A_3$R CRE-SPAP data and internalization data were fitted to the following equation:

$$Response = \frac{E_{max} \times [A]}{[A] + EC_{50}}$$

where $E_{max}$ is the maximal response, [A] is the concentration of agonist and the $EC_{50}$ is the molar concentration of agonist required to generate 50% of the $E_{max}$. Due to the two component nature of the $A_1$R CRE-SPAP data, the following equation was used:

$$Response = basal + (FK - basal)\left[1 - \frac{[A]}{([A] + IC_{50})}\right] + S_{MAX}\left[\frac{[A]}{([A] + EC_{50})}\right]$$

where basal is the response in the absence of agonist, FK is the response to 3 μM FSK in the absence of agonist, $IC_{50}$ is the concentration of agonist that inhibits 50% of the FSK response, $S_{MAX}$ is the maximal stimulation of the second component of the curve and $EC_{50}$ is for the second component of the curve and is the concentration of agonist that gives half the maximal stimulation.

## 3. Results

Four new fluorescent ABEA derivatives were synthesized in this study (Fig. 1; refer to Supplementary data for details). Previously, the adenosine receptor fluorescent agonist, ABEA-X-BY630 had been developed (Middleton et al., 2007), but this had poor imaging properties in long term studies due high levels of non-specific cytoplasmic uptake. In an effort to improve this fluorescent agonist, we incorporated a peptidic linker as an extra entity between the pharmacophore and the fluorophore. Glycine (gly) was selected as the *C*-terminal amino acid to enable successful racemization free segment coupling to the ABEA pharmacophore in solution-phase. Alanine-alanine (ala-ala) was used to provide a simple peptidic linker (ala-ala-gly; A-A-G), which also allowed examination of the importance of stereochemistry in the peptide linker. To this end, all four possible combinations of *L*- and *D*-ala were used in this ala-ala dipeptide part of the linker (BY630-X-(*L*)-A-(*L*)-A-G-ABEA, BY630-X-(*L*)-A-(*D*)-A-G-ABEA, BY630-X-(*D*)-A-(*L*)-A-G-ABEA, BY630-X-(*D*)-A-(*D*)-A-G-ABEA).

Using CHO cells lines containing a SPAP reporter gene linked to a CRE promoter (Baker et al., 2002) and expressing each of the four adenosine receptor subtypes ($A_1$R, $A_{2A}$R, $A_{2B}$R and $A_3$R) the potency and efficacy of the four fluorescent agonists was examined in relation to NECA. All four compounds retained a degree of potency at each of the adenosine receptors (Fig. 2, Table 1). The $A_{2A}$R and $A_{2B}$R are coupled to $G_s$, therefore an increase in the CRE-SPAP response was observed with agonist treatment. As the $A_3$R is $G_{i/o}$ coupled, FSK was added to increase the levels of CRE-SPAP via activation of adenylate cyclase, and agonist activation of the receptor resulted in a decrease of the FSK stimulated CRE-SPAP production. The $A_1$R also predominantly couples through $G_{i/o}$ but in this CRE-SPAP system a biphasic response is observed, with an inhibition of FSK stimulated CRE-SPAP at low agonist concentrations and an increase in signal over the FSK response at higher agonist concentrations and this has been previously shown to be through coupling to $G_s$ (Baker and Hill, 2007). At the $A_3$R all four of the compounds showed an increase in potency in comparison to NECA, and at $A_1$R all compounds, apart from BY630-X-(*L*)-A-(*L*)-A-G-ABEA, also showed a higher potency than NECA. BY630-X-(*D*)-A-(*L*)-A-G-ABEA was the most potent at both the $A_3$R and $A_1$R although there was no significant difference in potency in comparison to the potency of BY630-X-(*D*)-A-(*D*)-A-G-ABEA and BY630-X-(*L*)-A-(*D*)-A-G-ABEA. Whereas, at both $A_{2A}$R and $A_{2B}$R, all four compounds showed reduced potency when compared to NECA, with BY630-X-(*D*)-A-(*L*)-A-G-ABEA being the most potent at both receptors and BY630-X-(*L*)-A-(*L*)-A-G-ABEA showed the biggest reduction in potency (Fig. 2 and Table 1).

As the CRE-SPAP system is a well-coupled system that displayed a high degree of amplification, BY630-X-(*D*)-A-(*D*)-A-G-ABEA was selected for further testing in an additional functional assay with lower levels of receptor reserve. We chose to examine the ability of BY630-X-(*D*)-A-(*D*)-A-G-ABEA to stimulate the internalization of $A_1$-GFP and $A_3$-YFP using an ImageXpress Ultra confocal plate reader to automatically acquire the images. Treatment of cells expressing $A_1$-GFP or $A_3$-YFP with BY630-X-(*D*)-A-(*D*)-A-G-ABEA stimulated the internalization of both receptors as seen by the presence of intracellular accumulation of the labelled receptor (Fig. 3). Quantification of the images obtained was performed using an algorithm to detect granules and it was found that BY630-X-(*D*)-A-(*D*)-A-G-ABEA was more potent than NECA at $A_3$-YFP (NECA $pEC_{50}$ = 6.12 ± 0.23, BY630-X-(*D*)-A-(*D*)-A-G-ABEA $pEC_{50}$ = 7.47 ± 0.11, $n$ = 4). Whereas at $A_1$-GFP, BY630-X-(*D*)-A-(*D*)-A-G-ABEA stimulated receptor internalization with a similar potency to NECA (NECA $pEC_{50}$ = 5.52 ± 0.10, BY630-X-(*D*)-A-(*D*)-A-G-ABEA $pEC_{50}$ = 5.57 ± 0.10, $n$ = 3).

As BY630-X-(*D*)-A-(*D*)-A-G-ABEA was the most potent at $A_3$R compared to the other adenosine receptor subtypes in both functional assays, it was selected for imaging studies to investigate its use as a tool to localize adenosine receptors in living cells. To confirm that this fluorescent agonist had good imaging properties, cells stably expressing $A_3$-YFP were treated with 100 nM of BY630-X-(*D*)-A-(*D*)-A-G-ABEA at 37 °C in the presence and absence of a high concentration on unlabelled antagonist (1 μM MRS1220, 30 min) and imaged after 5 min or 60 min of agonist treatment (Fig. 4). After 5 min of agonist treatment, the fluorescence corresponding to BY630-X-(*D*)-A-(*D*)-A-G-ABEA is mainly localized at

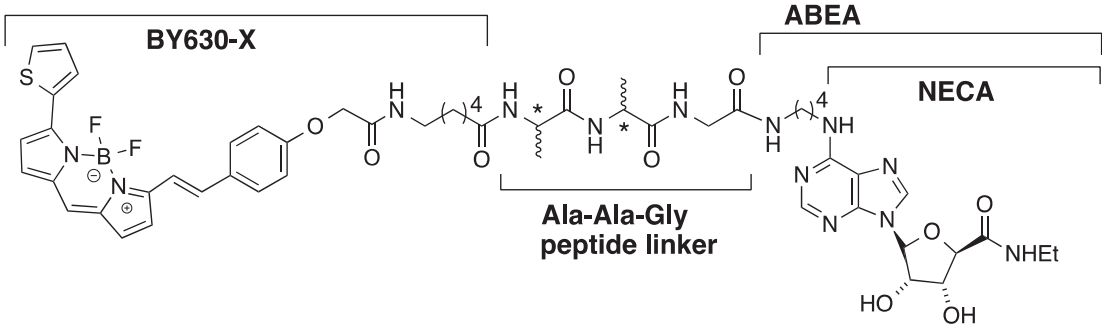


**Fig. 1.** Chemical structures of fluorescent NECA derivatives.

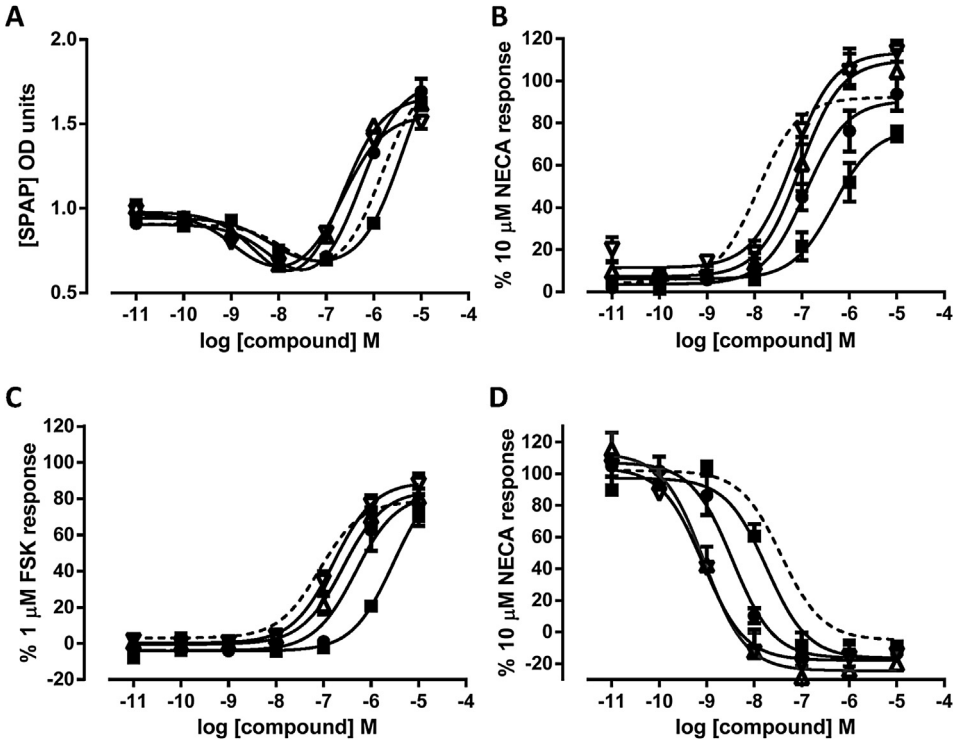


**Fig. 2.** Pharmacological evaluation of fluorescent ABEA derivatives at the four adenosine receptor subtypes in the CRE-SPAP gene transcription assay. The effect of the BY630-X-(*D*)-A-(*D*)-A-G-ABEA (●), BY630-X-(*L*)-A-(*L*)-A-G-ABEA (■), BY630-X-(*L*)-A-(*D*)-A-G-ABEA (△) and BY630-X-(*D*)-A-(*L*)-A-G-ABEA (▽) were assessed in $A_1R$ (**A**), $A_{2A}R$ (**B**), $A_{2B}R$ (**C**) and $A_3R$ (**D**) CRE-SPAP CHO cells. The response to the reference agonist, NECA, is shown as a dotted line. $A_1R$ cells and $A_3R$ cells were pre-treated with the fluorescent compounds for 30 min prior to the addition of 3 μM FSK for $A_1R$ cells and 1 μM FSK for $A_3R$ cells for 5 h. Compounds were added directly to $A_{2A}R$ and $A_{2B}R$ cells for 5 h. Data points in **A** represent mean ± SEM of one experiment performed in triplicate and is representative of four experiments. Data points in **B**, **C**, and **D** represent mean ± SEM of four experiments performed in triplicate.

**Table 1**
Potencies of fluorescent ABEA derivatives at the four adenosine receptor subtypes.

| Compound | $A_1R$ | | | | $A_{2A}R$ | | | $A_{2B}R$ | | | $A_3R$ | | |
|---|---|---|---|---|---|---|---|---|---|---|---|---|---|
| | $G_i$ | | $G_s$ | | | | | | | | | | |
| | $pEC_{50}$ | *n* | $pEC_{50}$ | *n* | $pEC_{50}$ | Efficacy | *n* | $pEC_{50}$ | Efficacy | *n* | $pEC_{50}$ | Efficacy | *n* |
| NECA | 8.31 ± 0.18 | 4 | 5.73 ± 0.14 | 4 | 7.70 ± 0.23 | 100 | 4 | 7.17 ± 0.11 | 100 | 4 | 7.61 ± 0.16 | 100 | 4 |
| BY630-X-(*D*)-A-(*D*)-A-G-ABEA | 8.77 ± 0.22 | 4 | 5.92 ± 0.19 | 4 | 6.81 ± 0.17 | 93.7 ± 7.9 | 4 | 6.30 ± 0.11 | 89.9 ± 11.2 | 4 | 8.48 ± 0.09 | 113.6 ± 3.4 | 4 |
| BY630-X-(*L*)-A-(*L*)-A-G-ABEA | 8.16 ± 0.07 | 4 | 5.58 ± 0.34 | 4 | 6.33 ± 0.28 | 75.0 ± 3.4 | 4 | 5.51 ± 0.14 | 84.6 ± 10.0 | 4 | 7.75 ± 0.14 | 110.6 ± 4.7 | 4 |
| BY630-X-(*L*)-A-(*D*)-A-G-ABEA | 8.89 ± 0.30 | 4 | 6.71 ± 0.08 | 4 | 7.02 ± 0.14 | 104.4 ± 10.4 | 4 | 6.55 ± 0.12 | 77.5 ± 5.3 | 4 | 9.05 ± 0.12 | 120.1 ± 6.5 | 4 |
| BY630-X-(*D*)-A-(*L*)-A-G-ABEA | 9.00 ± 0.12 | 4 | 6.91 ± 0.10 | 4 | 7.18 ± 0.08 | 114.1 ± 5.0 | 4 | 6.75 ± 0.09 | 84.1 ± 4.6 | 4 | 9.10 ± 0.19 | 113.7 ± 7.7 | 4 |

The $pEC_{50}$ values were determined in CHO CRE-SPAP cells expressing $A_1R$, $A_{2A}R$, $A_{2B}R$ or $A_3R$. Values are mean ± SEM from 4 separate experiments. For $A_1R$ values are $pIC_{50}$ and $pEC_{50}$ from the inhibition ($G_i$) and stimulation ($G_s$) respectively of FSK-stimulated CRE-SPAP activity. For $A_{2A}R$ and $A_{2B}R$ $pEC_{50}$ were determined from the direct stimulation of CRE-SPA P activity and for $A_3R$ the $pIC_{50}$ values were determined from the inhibition of FSK stimulated CRE-SPAP production.

the surface of the cells with little intracellular fluorescence and this membrane localization corresponds to the expression of $A_3R$ as visualized by the YFP fluorescence. Treatment with MRS1220 substantially reduces binding of BY630-X-(*D*)-A-(*D*)-A-G-ABEA as seen by a reduction in the membrane BY630 fluorescence and this antagonist treatment had no effect on the localization of the receptor as the YFP fluorescence was still predominately membrane localized. After 60 min of agonist treatment, there was a reduction in the membrane $A_3$-YFP fluorescence and an increase in the intracellular fluorescence corresponding to internalized clusters of receptor. Importantly, there was a high degree of co-localization of the BY630 fluorescence with the $A_3$-YFP fluorescence indicating that BY630-X-(*D*)-A-(*D*)-A-G-ABEA was internalised with the receptor. Importantly, even after 60 min of agonist treatment the presence of an unlabelled antagonist blocked the internalization of the receptor and the binding of BY630-X-(*D*)-A-(*D*)-A-G-ABEA (Fig. 4). In addition, there were low levels of non-specific cytoplasmic fluorescence after 60 min treatment with BY630-X-(*D*)-A-(*D*)-A-G-ABEA in both the presence and absence of MRS1220. It is also important to note that these experiments were performed in the continued presence of the fluorescence agonist and there was no requirement for a wash step to observe specific fluorescence from the labelled agonist.

Since the labelling of the $A_3$-YFP receptor with BY630-X-(*D*)-A-(*D*)-A-G-ABEA appeared very specific, it was possible to use this fluorescence ligand to investigate the internalization of unlabelled receptor using CHO cells stably expressing the wild type human $A_3R$. After 5 min of exposure to 100 nM BY630-X-(*D*)-A-(*D*)-A-G-ABEA there was predominately cell surface localization of the BY630 fluorescence and this was abolished by pre-treatment of the cells with 1 μM MRS1220, indicating that the fluorescence observed was $A_3R$ specific (Fig. 5). After 60 min of agonist treatment, there

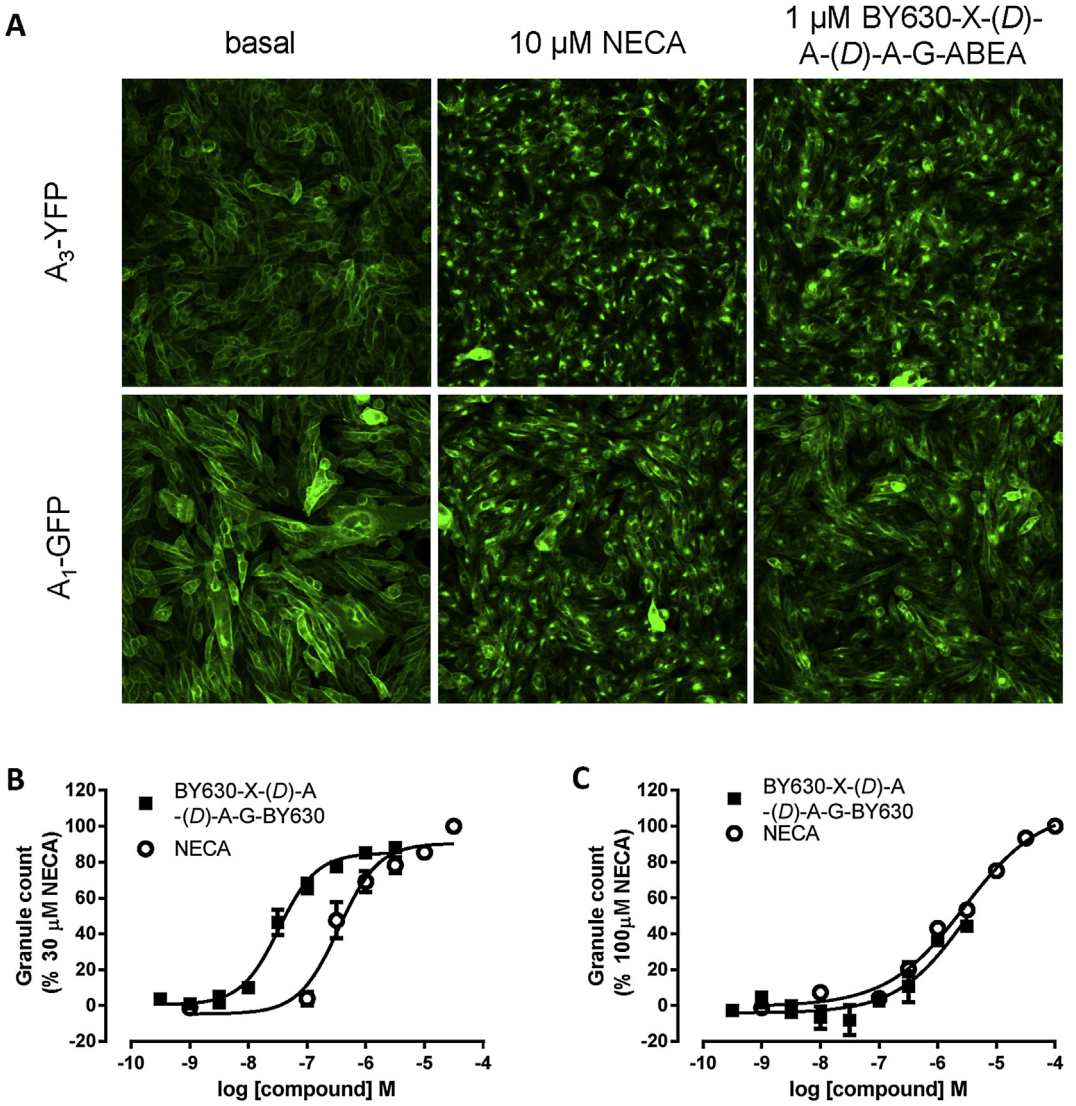


**Fig. 3.** BY630-X-(*D*)-A-(*D*)-A-G-ABEA stimulated internalization of $A_1$-GFP and $A_3$-YFP. CHO cells expressing $A_1$-GFP or $A_3$-YFP were stimulated with increasing concentrations of NECA or BY630-X-(*D*)-A-(*D*)-A-G-ABEA for 1 h prior to automated confocal image capture and analysis on the ImageXpress Ultra plate reader. (**A**) Representative images of untreated (left hand panels), 10 μM NECA (middle panels) and 1 μM BY630-X-(*D*)-A-(*D*)-A-G-ABEA (right hand panels) treated $A_3$-YFP (top panels) and $A_1$-GFP (bottom panels) cells. Images are representative of those obtain in four ($A_3$-YFP) and three ($A_1$-GFP) experiments. Concentration dependent increase in granule count in $A_3$-YFP (**B**) and $A_1$-GFP (**C**) cells treated with NECA (open circles) or BY630-X-(*D*)-A-(*D*)-A-G-ABEA (squares). The data show represent granule count per cell and are represented as a percentage as the 30 μM NECA (B) or 100 μM NECA (C) responses. Each data point represents mean ± SEM of four (B) and three (C) experiments performed in triplicate.

was still some membrane localization of the fluorescence corresponding to BY630-X-(*D*)-A-(*D*)-A-G-ABEA, there was also an increase in intracellular BY630 fluorescence with some degree of clustering of the fluorescence into granules. Again, pre-treatment of the cells with 1 μM MRS1220 prevented the binding of BY630-X-(*D*)-A-(*D*)-A-G-ABEA (Fig. 5) demonstrating that the intracellular accumulation of the fluorescent ligand was a result of receptor internalization.

Receptor internalization in response to agonist treatment is mediated through the phosphorylation of the receptor by G protein receptor kinases, the binding of arrestins and the subsequent removal from the cell membrane via clathrin coated pits. To further confirm that BY630-X-(*D*)-A-(*D*)-A-G-ABEA is mediating the internalization of the $A_3$R and co-localizing with these internalized receptor, a bimolecular fluorescence complementation (BiFC) approach was used. BiFC detects an interaction between two non-fluorescent fragments of venusYFP (vYFP) which are attached to $A_3$R and arrestin3, respectively. Interaction of the two labelled proteins allows recombination of vYFP chromophore from the fragments and its subsequent visualization. As this is an essentially irreversible process any vYFP fluorescence detected corresponds to $A_3$R-arrestin3 complexes. Treatment with BY630-X-(*D*)-A-(*D*)-A-G-ABEA for 5 min in the absence of MRS1220 resulted in plasma membrane binding of the fluorescent ligand with some small granules of fluorescence within the cells and this corresponded to a clustering of the vYFP fluorescence (Fig. 6). Visualization of CHO cells stably expressing $A_3$-vYc and arrestin3-vYnL with BY630-X-(*D*)-A-(*D*)-A-G-ABEA for 5 min at 37 °C after pre-treatment with 1 μM MRS1220 showed low levels of vYFP fluorescence that were mainly localized to the plasma membrane, with very little BY630 fluorescence. After 60 min of treatment with the fluorescent agonist, the BiFC fluorescence is highly concentrated within the cells with very little vYFP fluorescence at the plasma membrane. The equivalent images of BY630-X-(*D*)-A-(*D*)-A-G-ABEA also showed a clustering of the fluorescence within the cell and a high degree of co-localization of this with the vYFP fluorescence. There

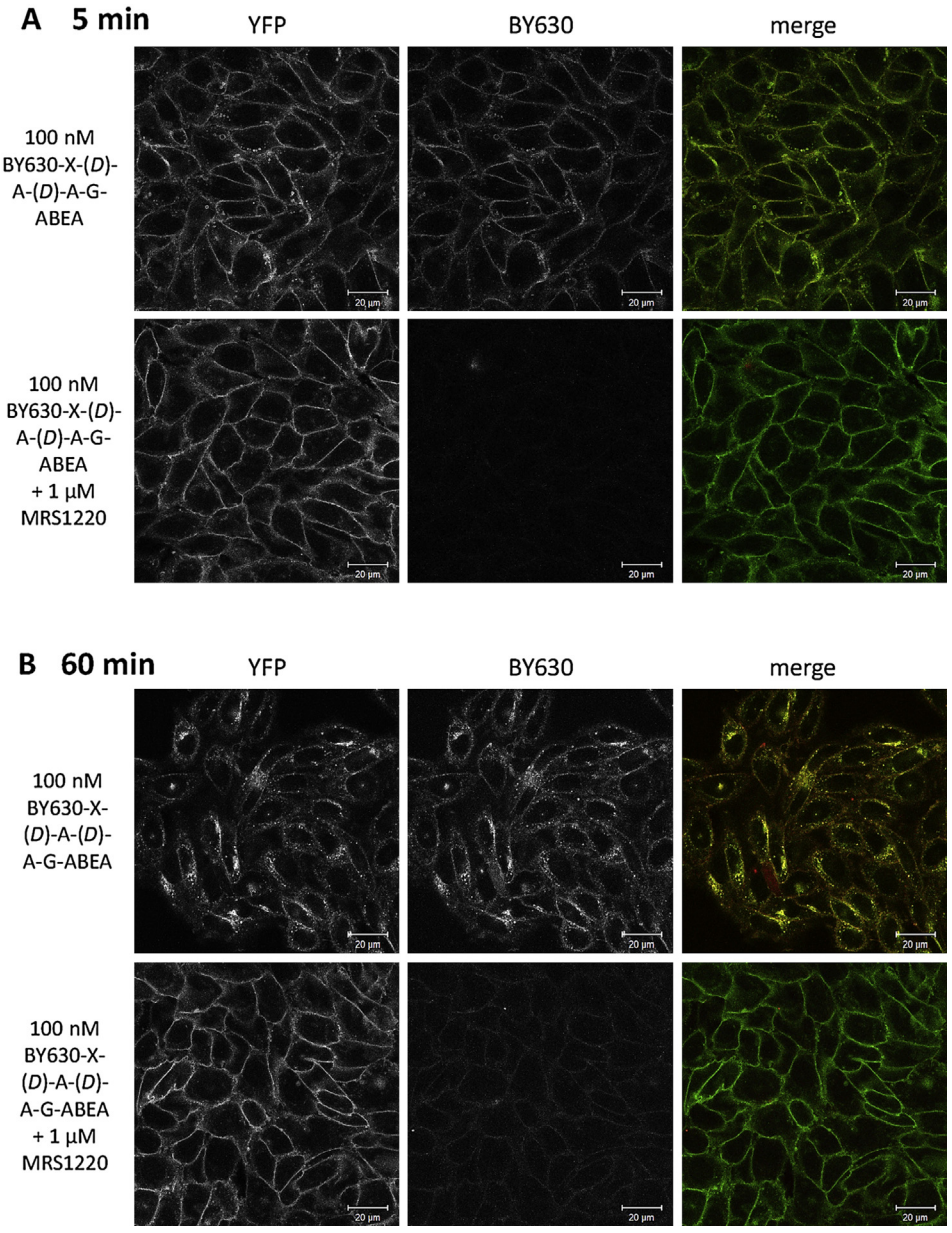


**Fig. 4.** Co-localization of BY630-X-(*D*)-A-(*D*)-A-G-ABEA with internalized $A_3$-YFP. Confocal images of cells expressing $A_3$-YFP and incubated with 100 nM BY630-X-(*D*)-A-(*D*)-A-G-ABEA for 5 min (**A**) and 60 min (**B**) at 37 °C in the absence (top panels) or presence of 1 μM MRS1220 (bottom panels). Images were obtained in the continued presence of BY630-X-(*D*)-A-(*D*)-A-G-ABEA. Single equatorial images were taken showing the YFP (left hand panels) and BY630 (middle panels). YFP and BY630 images are shown in grayscale to avoid issues with colour rendering. Images in the right hand panels represent the merge of the YFP and BY630 images. Data shown are representative of images taken in four independent experiments, with all images within one experiment taken with identical microscope settings.

is also some clear residual membrane binding of the BY630-X-(*D*)-A-(*D*)-A-G-ABEA which is likely to be binding to receptor which is not associated with arrestin3. Again, pre-treatment of the cells with 1 μM MRS1220 prior to the 60 min incubation with BY630-X-(*D*)-A-(*D*)-A-G-ABEA prevents the binding of the fluorescent agonist, the resulting increase in vYFP fluorescence and the redistribution of the receptor (Fig. 6).

## 4. Discussion

Fluorescent ligands for GPCRs are valuable tools to study the localization of receptors in their native environment and to answer important questions on their pharmacology. To enable their use in the study of GPCRs, the pharmacological, spectral and imaging properties of the ligand need to be optimized for specific applications. In this study, our aim was to generate new fluorescent agonists to study the cellular localization of adenosine receptors. This was achieved by incorporating peptide linkers into an existing fluorescent adenosine receptor agonist ABEA-X-BY630 (Middleton et al., 2007) based on a strategy which has been successfully employed with adenosine receptor fluorescent antagonists (Vernall et al., 2013) and which resulted in fluorescent XAC derivatives with improved imaging properties. In the present study, four different ala-ala-gly tripeptide linkers were incorporated between the NECA derivative, ABEA, and the BY630 fluorophore to generate four fluorescent agonists containing each of the possible combinations

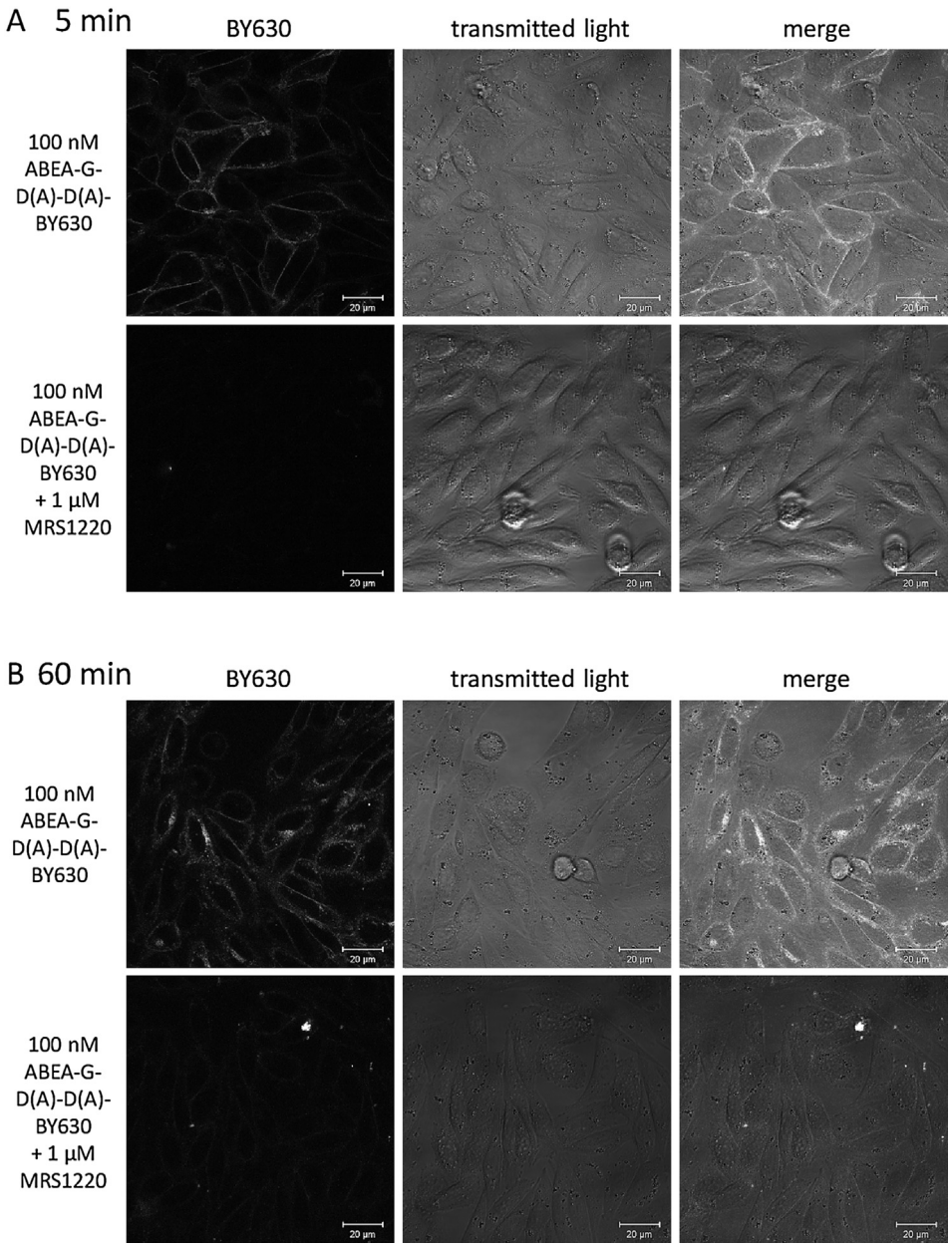


**Fig. 5.** Visualization of BY630-X-(*D*)-A-(*D*)-A-G-ABEA stimulated internalization of $A_3$AR. In each case the left panel shows confocal images, while the middle panel shows the transmitted light image of the same field of cells. $A_3$R receptor expressing CHO cells were treated with 100 nM BY630-X-(*D*)-A-(*D*)-A-G-ABEA at 37 °C for 5 min (**A**) or 60 min (**B**) in the presence (top panels) or absence (bottom panels) of 1 μM MRS1220 prior to the capture of the single equatorial confocal images of the BY630 fluorescence and the transmitted light images. Images shown are representative of images taken in four independent experiments.

of amino acid stereochemistry (BY630-X-(*D*)-A-(*D*)-A-G-ABEA, BY630-X-(*L*)-A-(*L*)-A-G-ABEA, BY630-X-(*L*)-A-(*D*)-A-G-ABEA and BY630-X-(*D*)-A-(*L*)-A-G-ABEA). Although NECA is not selective between the four adenosine receptor subtypes, the new peptide-linked fluorescent compounds showed significantly higher potency at the $A_1$R and $A_3$R in comparison to the $A_{2A}$R and $A_{2B}$R indicating that the length and composition of the peptide linker may play a role in interacting differently with the different receptor subtypes. This is further confirmed by the differences in the affinity of the stereoisomers as the rank order of the four fluorescent compounds was roughly the same at all four adenosine receptors. The significance of the linker region in generating high affinity and high potency fluorescent ligands has been previously observed for the adenosine $A_1$ (Baker et al., 2010) and $A_3$ receptors (Vernall et al., 2013), the β adrenergic receptors (Baker et al., 2011), the oxytocin receptor (Karpenko et al., 2014) and the dopamine $D_2$ receptor (Hounsou et al., 2015) and this present study confirms the importance of the linker as an integral part in the design of fluorescent GPCR ligands.

It was also important to consider the imaging properties of the newly synthesized fluorescent agonist; high affinity or potency does not necessarily equate to specific cell surface imaging (Rose et al., 2012). The incorporation of the peptide linkers into these adenosine receptor fluorescent agonists resulted in ligands that showed specific membrane binding in cells expressing the $A_3$R. This specific imaging was seen in the continued presence of the fluorescent agonist which is in contrast to previously described fluorescent agonist for the adenosine receptors. Kozma and co-workers

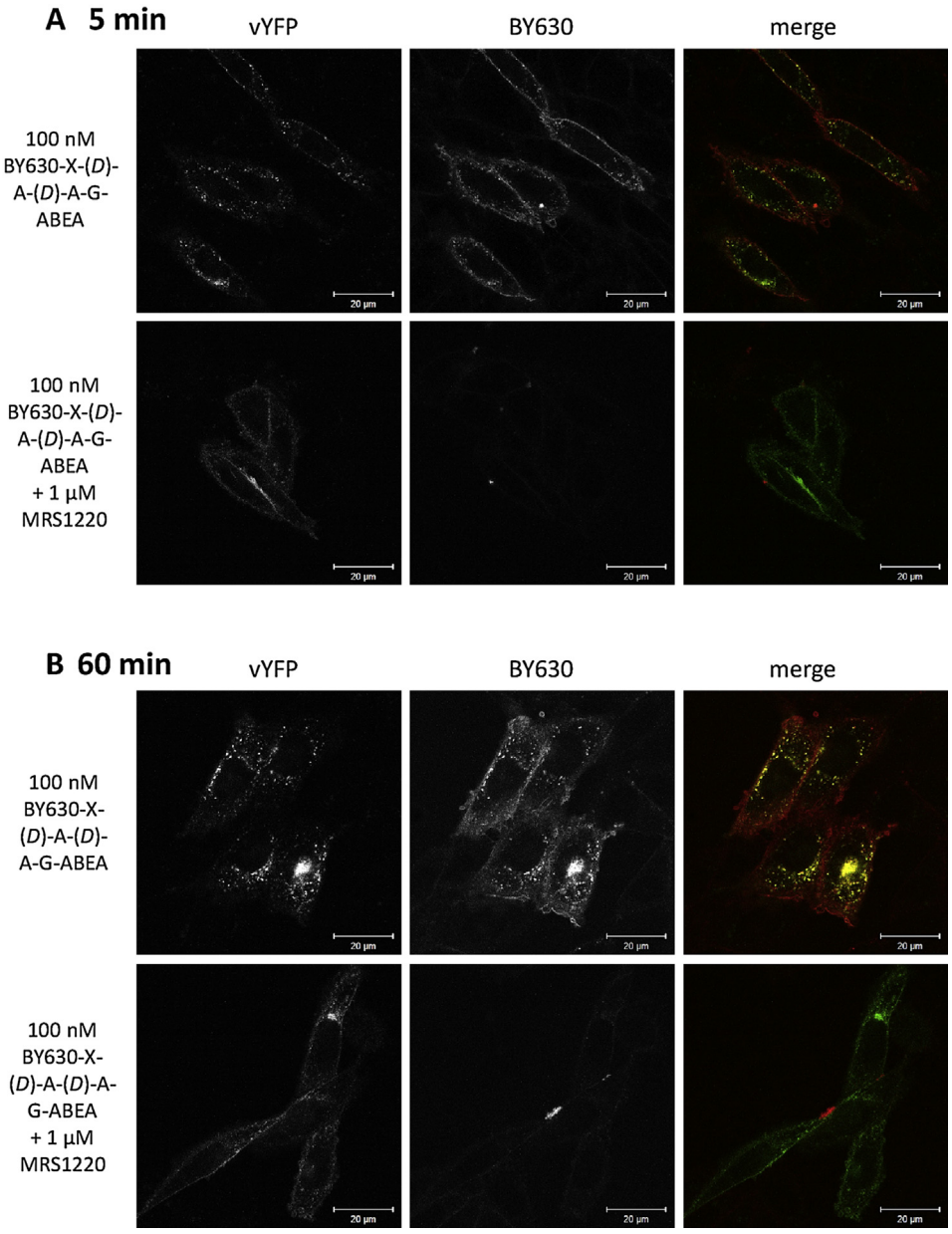


**Fig. 6.** Co-localization of BY630-X-(*D*)-A-(*D*)-A-G-ABEA with $A_3$/arrestin3 BiFC complexes. CHO cells co-expressing $A_3$-vYc and arrestin3-vYnL were treated with and without 1 μM MRS1220 for 30 min prior to any agonist treatment. Cell were then treated with 100 nM BY630-X-(*D*)-A-(*D*)-A-G-ABEA at 37 °C for 5 min (**A**) or 60 min (**B**) in the presence or absence of 1 μM MRS1220 and confocal images obtained. The left hand panels represent vYFP fluorescence, middle panels BY630 fluorescence and right hand panels the merge of vYFP and BY630 images. vYFP and BY630 images are shown in grayscale to avoid issues with colour rendering. Images shown are representative of those taken in four independent experiments.

used the Cy5 labelled $A_3$R selective agonist, MRS5218 (Tosh et al., 2009), and showed accumulation of this agonist within $A_3$R expressing cells which they attributed to receptor internalization, although they did not block this internalization with unlabelled ligand and they required the removal of excess fluorescent ligand to generate confocal images (Kozma et al., 2013a). In addition, it has been shown for the adenosine $A_{2A}$ receptors that a fluorescent agonist, Alexa488-APEC, could stimulate the internalization of CFP tagged receptor and that the fluorescent ligand was co-localized with this internalized receptor, although these images were obtained after removal of excess fluorescent ligand (Brand et al., 2008). The ability to measure binding of BY630 labelled compounds in the continued presence of the ligand has been observed for adenosine receptor antagonists (Baker and Hill, 2007; Stoddart et al., 2012; Vernall et al., 2012) and agonists (May et al., 2010) and $\beta_2$ adrenoceptor antagonists (Baker et al., 2011). The quantum yield of fluorescent adenosine receptor antagonists containing the BY630 fluorophore have been shown to increase in non-aqueous environments (Baker et al., 2010) suggesting that the high levels of fluorescence observed with BY630-X-(*D*)-A-(*D*)-A-G-ABEA indicate that it is a non-polar environment when bound to the $A_3$R. This non-polar environment is expected to be the plasma membrane and modelling studies of $A_3$R fluorescent antagonists supports the idea that the flurophore is within the lipid bilayer (Vernall et al., 2013). Fluorescent ligands for the oxytocin receptor using Nile Red as the fluorophore have recently been developed which also display high levels of fluorescence in a non-aqueous environment (Karpenko et al., 2014).

Using BY630-X-(*D*)-A-(*D*)-A-G-ABEA we have shown that the fluorescent agonist is in close proximity to the receptor upon sequestration of the receptor from the plasma membrane. Using fluorescent ligands, it has been suggested that the agonist remains bound to the adenosine $A_{2A}$ (Brand et al., 2008) and $A_3$ receptors (Kozma et al., 2013a) upon internalization. Upon activation by agonist, the $A_3$R receptor has been shown to be phosphorylated at the C-terminus by GRKs (Ferguson et al., 2000; Palmer and Stiles, 2000) which leads to internalization via clathrin coated pits (Trincavelli et al., 2000). It is unclear if this clathrin dependent mechanism of internalization is dependent of arrestin recruitment as in the rat basophilic leukaemia 2H3 cell line (RBL-2H3) which endogenously express arrestin2, 3 and the $A_3$R, no recruitment of arrestin upon agonist stimulation of $A_3$R could be detected (Santini et al., 2000) and there was no co-localization of arrestin3 and $A_3$R in HEK293 cells transiently expressing both proteins (Ferguson et al., 2002). We have previously shown that $A_3$R can associate with arrestin3 in a concentration-dependent manner in a BiFC assay (Stoddart et al., 2014). In the present study, we have additionally showed that the fluorescent agonist co-localizes with $A_3$R-arrestin3 complexes as visualized by BiFC. This may be due to the fact that BiFC traps the receptor-β arrestin complex, as the association of the two halves of venusYFP is essentially irreversible (Morell et al., 2007). The presence of an agonist-receptor-arrestin complex has been suggested previously through the presence of high affinity agonist sites (Gurevich et al., 1997) but we believe this is the first study to directly visualize this complex through the use of a fluorescent agonist. The ability to image agonist-receptor-arrestin complex raises the possibility to track agonist–receptor complex throughout the internalization, degradation and recycling processes. Using a biosensor based on a nanobody that only recognises the active conformation of the $\beta_2$AR, Irannejad et al. (2013) recently showed that internalized receptor was still an active confirmation as seen by continued binding of the antibody. This internalized receptor could continue to signal through the cAMP pathway, although they were unable to confirm if the agonist was still bound to the receptor (Irannejad et al., 2013). By showing that BY630-X-(*D*)-A-(*D*)-A-G-ABEA localizes with a receptor–arrestin complex, this supports the idea that agonists are still bound to the internalized receptor and sequestration from the plasma membrane may not lead to the direct termination of agonist-induced signalling (Calebiro et al., 2010). The use of fluorescent agonists that can be imaged without wash steps may help to elucidate the precise point in which the agonist and receptor are no longer bound and termination of agonist induced signalling occurs.

We have shown that BY630-X-(*D*)-A-(*D*)-A-G-ABEA can be used to visualize the internalization of untagged receptors, and that this method does not need an further additional chemical modification of the receptor. The presence of a fluorescent protein or epitope tag on a receptor expressed in a host cell can bias the selection of cells that highly express the receptor during generation of the cell line. It is therefore important to confirm in cell lines where the receptor expression level is unknown, and only inferred from functional assays, that receptor internalization can still be visualized with the fluorescent agonist as a first step towards using this tool in a system that endogenously expresses adenosine receptors. This has previously been achieved for the μ opioid receptor, through the use of fluorescently labelled dermorphin, to study internalization of endogenously expressed receptors in primary neurons (Arttamangkul et al., 2006). The $A_3$ receptor is present in various tissues with particularly high levels of expression in various cells of the immune system, including the microglia and astrocytes (Bjorklund et al., 2008; Ohsawa et al., 2012; van der Putten et al., 2009). In addition expression of the $A_3$ receptor has been detected in various areas of the brain including thalamus, hypothalamus (Yaar et al., 2002) and at motor nerve terminals (Cinalli et al., 2013). We have also recently shown, using a fluorescent adenosine receptor antagonist, that the $A_3$ receptor can be found in discrete microdomains on human neutrophils which are located at the bottom of membrane projections (Corriden et al., 2013).

In conclusion, we have demonstrated that BY630-X-(*D*)-A-(*D*)-A-G-ABEA is a highly potent agonist of the $A_3$ receptor which can be used to visualize the internalization of the receptor. In addition, we have shown that the fluorescent agonist co-localizes with internalized receptor-arrestin complexes. The development of this highly specific fluorescent probe will help to understand the regulation of the receptor with future studies and to investigate the role of the receptor in endogenously expressing systems.

## Acknowledgements

We thank the Medical Research Council for financial support (G0800006), Monica Mistry for help with synthesis of BY630-X-(*D*)-A-(*D*)-A-G-ABEA and Nigel Birdsall for kindly providing us with the CHO $A_1$-GFP cell line.

## Appendix A. Supplementary data

Supplementary data related to this article can be found at http://dx.doi.org/10.1016/j.neuropharm.2015.04.013.

## References

Arttamangkul, S., Torrecilla, M., Kobayashi, K., Okano, H., Williams, J.T., 2006. Separation of μ-opioid receptor desensitization and internalization: endogenous receptors in primary neuronal cultures. J. Neurosci. 26 (15), 4118–4125.

Baker, J.G., Adams, L.A., Salchow, K., Mistry, S.N., Middleton, R.J., Hill, S.J., Kellam, B., 2011. Synthesis and characterization of high-affinity 4, 4-Difluoro-4-bora-3a,4a-diaza-s-indacene-labeled fluorescent ligands for human beta-adrenoceptors. J. Med. Chem. 54 (19), 6874–6887.

Baker, J.G., Hall, I.P., Hill, S.J., 2002. Pharmacological characterization of CGP 12177 at the human beta(2)-adrenoceptor. Br. J. Pharmacol. 137 (3), 400–408.

Baker, J.G., Hill, S.J., 2007. A comparison of the antagonist affinities for the Gi- and Gs-coupled states of the human adenosine A1-receptor. J. Pharmacol. Exp. Ther. 320 (1), 218–228.

Baker, J.G., Middleton, R., Adams, L., May, L.T., Briddon, S.J., Kellam, B., Hill, S.J., 2010. Influence of fluorophore and linker composition on the pharmacology of fluorescent adenosine A(1) receptor ligands. Br. J. Pharmacol. 159 (4), 772–786.

Bjorklund, O., Shang, M., Tonazzini, I., Dare, E., Fredholm, B.B., 2008. Adenosine A1 and A3 receptors protect astrocytes from hypoxic damage. Eur. J. Pharmacol. 596 (1–3), 6–13.

Boutin, A., Allen, M.D., Neumann, S., Gershengorn, M.C., 2012. Persistent signaling by thyrotropin-releasing hormone receptors correlates with G-protein and receptor levels. FASEB J. 26 (8), 3473–3482.

Brand, F., Klutz, A.M., Jacobson, K.A., Fredholm, B.B., Schulte, G., 2008. Adenosine A(2A) receptor dynamics studied with the novel fluorescent agonist Alexa488-APEC. Eur. J. Pharmacol. 590 (1–3), 36–42.

Calebiro, D., Nikolaev, V.O., Persani, L., Lohse, M.J., 2010. Signaling by internalized G-protein-coupled receptors. Trends Pharmacol. Sci. 31 (5), 221–228.

Chen, J.F., Eltzschig, H.K., Fredholm, B.B., 2013. Adenosine receptors as drug targets – what are the challenges? Nat. Rev. Drug Discov. 12 (4), 265–286.

Chen, J.F., Sonsalla, P.K., Pedata, F., Melani, A., Domenici, M.R., Popoli, P., Geiger, J., Lopes, L.V., de Mendonca, A., 2007. Adenosine A2A receptors and brain injury: broad spectrum of neuroprotection, multifaceted actions and "fine tuning" modulation. Prog. Neurobiol. 83 (5), 310–331.

Cinalli, A.R., Guarracino, J.F., Fernandez, V., Roquel, L.I., Losavio, A.S., 2013. Inosine induces presynaptic inhibition of acetylcholine release by activation of A3 adenosine receptors at the mouse neuromuscular junction. Br. J. Pharmacol. 169 (8), 1810–1823.

Corriden, R., Self, T., Akong-Moore, K., Nizet, V., Kellam, B., Briddon, S.J., Hill, S.J., 2013. Adenosine-A3 receptors in neutrophil microdomains promote the formation of bacteria-tethering cytonemes. EMBO Rep. 14 (8), 726–732.

Ferguson, G., Watterson, K.R., Palmer, T.M., 2000. Subtype-specific kinetics of inhibitory adenosine receptor internalization are determined by sensitivity to phosphorylation by G protein-coupled receptor kinases. Mol. Pharmacol. 57 (3), 546–552.

Ferguson, G., Watterson, K.R., Palmer, T.M., 2002. Subtype-specific regulation of receptor internalization and recycling by the carboxyl-terminal domains of the human A1 and rat A3 adenosine receptors: consequences for agonist-stimulated translocation of arrestin3. Biochemistry 41 (50), 14748–14761.

Fredholm, B.B., AP, I.J., Jacobson, K.A., Klotz, K.N., Linden, J., 2001. International Union of Pharmacology. XXV. Nomenclature and classification of adenosine receptors. Pharmacol. Rev. 53 (4), 527–552.
Gurevich, V.V., Pals-Rylaarsdam, R., Benovic, J.L., Hosey, M.M., Onorato, J.J., 1997. Agonist-receptor-arrestin, an alternative ternary complex with high agonist affinity. J. Biol. Chem. 272 (46), 28849–28852.
Hill, S.J., May, L.T., Kellam, B., Woolard, J., 2014. Allosteric interactions at adenosine A1 and A3 receptors: new insights into the role of small molecules and receptor dimerization. Br. J. Pharmacol. 171 (5), 1102–1113.
Hounsou, C., Margathe, J.F., Oueslati, N., Belhocine, A., Dupuis, E., Thomas, C., Mann, A., Ilien, B., Rognan, D., Trinquet, E., Hibert, M., Pin, J.P., Bonnet, D., Durrox, T., 2015. Time resolved FRET binding assay to investigate hetero-oligomer binding properties: proof of concept with dopamine D/D heterodimer. ACS Chem. Biol. 10 (2), 466–474.
Huang, Z.L., Urade, Y., Hayaishi, O., 2007. Prostaglandins and adenosine in the regulation of sleep and wakefulness. Curr. Opin. Pharmacol. 7 (1), 33–38.
Irannejad, R., Tomshine, J.C., Tomshine, J.R., Chevalier, M., Mahoney, J.P., Steyaert, J., Rasmussen, S.G., Sunahara, R.K., El-Samad, H., Huang, B., von Zastrow, M., 2013. Conformational biosensors reveal GPCR signalling from endosomes. Nature 495 (7442), 534–538.
Jenner, P., Mori, A., Hauser, R., Morelli, M., Fredholm, B.B., Chen, J.F., 2009. Adenosine, adenosine A2A antagonists, and Parkinson's disease. Park. Relat. Disord. 15 (6), 406–413.
Karpenko, I.A., Kreder, R., Valencia, C., Villa, P., Mendre, C., Mouillac, B., Mely, Y., Hibert, M., Bonnet, D., Klymchenko, A.S., 2014. Red fluorescent turn-on ligands for imaging and quantifying G protein-coupled receptors in living cells. Chembiochem 15 (3), 359–363.
Kenakin, T., 2012. The potential for selective pharmacological therapies through biased receptor signaling. BMC Pharmacol. Toxicol. 13, 3.
Kilpatrick, L.E., Briddon, S.J., Hill, S.J., Holliday, N.D., 2010. Quantitative analysis of neuropeptide Y receptor association with beta-arrestin2 measured by bimolecular fluorescence complementation. Br. J. Pharmacol. 160 (4), 892–906.
Kozma, E., Gizewski, E.T., Tosh, D.K., Squarcialupi, L., Auchampach, J.A., Jacobson, K.A., 2013a. Characterization by flow cytometry of fluorescent, selective agonist probes of the A3 adenosine receptor. Biochem. Pharmacol. 85 (8), 1171–1181.
Kozma, E., Jayasekara, P.S., Squarcialupi, L., Paoletta, S., Moro, S., Federico, S., Spalluto, G., Jacobson, K.A., 2013b. Fluorescent ligands for adenosine receptors. Bioorg. Med. Chem. Lett. 23 (1), 26–36.
May, L.T., Briddon, S.J., Hill, S.J., 2010. Antagonist selective modulation of adenosine A1 and A3 receptor pharmacology by the food dye brilliant black BN: evidence for allosteric interactions. Mol. Pharmacol. 77 (4), 678–686.
May, L.T., Bridge, L.J., Stoddart, L.A., Briddon, S.J., Hill, S.J., 2011. Allosteric interactions across native adenosine-A(3) receptor homodimers: quantification using single-cell ligand-binding kinetics. FASEB J. 25 (10), 3465–3476.
Middleton, R.J., Briddon, S.J., Cordeaux, Y., Yates, A.S., Dale, C.L., George, M.W., Baker, J.G., Hill, S.J., Kellam, B., 2007. New fluorescent adenosine $A_1$-receptor agonists that allow quantification of ligand–receptor interactions in microdomains of single living cells. J. Med. Chem. 50 (4), 782–793.
Morell, M., Espargaro, A., Aviles, F.X., Ventura, S., 2007. Detection of transient protein-protein interactions by bimolecular fluorescence complementation: the Abl-SH3 case. Proteomics 7 (7), 1023–1036.
Mullershausen, F., Zecri, F., Cetin, C., Billich, A., Guerini, D., Seuwen, K., 2009. Persistent signaling induced by FTY720-phosphate is mediated by internalized S1P1 receptors. Nat. Chem. Biol. 5 (6), 428–434.
Mundell, S.J., Luty, J.S., Willets, J., Benovic, J.L., Kelly, E., 1998. Enhanced expression of G protein-coupled receptor kinase 2 selectively increases the sensitivity of A2A adenosine receptors to agonist-induced desensitization. Br. J. Pharmacol. 125 (2), 347–356.
Mundell, S.J., Matharu, A.L., Kelly, E., Benovic, J.L., 2000. Arrestin isoforms dictate differential kinetics of A2B adenosine receptor trafficking. Biochemistry 39 (42), 12828–12836.
Nie, Z.Z., Mei, Y., Ramkumar, V., 1997. Short term desensitization of the A1 adenosine receptors in DDT1MF-2 cells. Mol. Pharmacol. 52 (3), 456–464.
Ohsawa, K., Sanagi, T., Nakamura, Y., Suzuki, E., Inoue, K., Kohsaka, S., 2012. Adenosine A3 receptor is involved in ADP-induced microglial process extension and migration. J. Neurochem. 121 (2), 217–227.
Ohta, A., Sitkovsky, M., 2001. Role of G-protein-coupled adenosine receptors in downregulation of inflammation and protection from tissue damage. Nature 414 (6866), 916–920.
Palmer, T.M., Gettys, T.W., Jacobson, K.A., Stiles, G.L., 1994. Desensitization of the canine A2A-adenosine receptor – delineation of multiple processes. Mol. Pharmacol. 45 (6), 1082–1094.
Palmer, T.M., Stiles, G.L., 2000. Identification of threonine residues controlling the agonist-dependent phosphorylation and desensitization of the rat A3 adenosine receptor. Mol. Pharmacol. 57 (3), 539–545.
Peters, D.M., Gies, E.K., Gelb, C.R., Peterfreund, R.A., 1998. Agonist-induced desensitization of A2B adenosine receptors. Biochem. Pharmacol. 55 (6), 873–882.
Ramkumar, V., Olah, M.E., Jacobson, K.A., Stiles, G.L., 1991. Distinct pathways of desensitization of adenosine-A1 and adenosine-A2 receptors in DDT1 MF-2 cells. Mol. Pharmacol. 40 (5), 639–647.
Rose, R.H., Briddon, S.J., Hill, S.J., 2012. A novel fluorescent histamine H1 receptor antagonist demonstrates the advantage of using fluorescence correlation spectroscopy to study the binding of lipophilic ligands. Br. J. Pharmacol. 165 (6), 1789–1800.
Santini, F., Penn, R.B., Gagnon, A.W., Benovic, J.L., Keen, J.H., 2000. Selective recruitment of arrestin-3 to clathrin coated pits upon stimulation of G protein-coupled receptors. J. Cell. Sci. 113 (Pt 13), 2463–2470.
Stoddart, L.A., Briddon, S.J., Hill, S.J., 2013. Fluorescent ligands for G protein-coupled receptors: illuminating receptor-ligand interactions for drug discovery. Future Med. Chem. 5 (12), 1367–1369.
Stoddart, L.A., Kellam, B., Briddon, S.J., Hill, S.J., 2014. Effect of a toggle switch mutation in TM6 of the human adenosine A3 receptor on Gi protein-dependent signalling and Gi-independent receptor internalization. Br. J. Pharmacol. 171 (16), 3827–3844.
Stoddart, L.A., Kilpatrick, L.E., Briddon, S.J., Hill, S.J., 2015. Probing the pharmacology of G protein-coupled receptors with fluorescent ligands. Neuropharmacol 98, 48–57.
Stoddart, L.A., Vernall, A.J., Denman, J.L., Briddon, S.J., Kellam, B., Hill, S.J., 2012. Fragment screening at adenosine-A3 receptors in living cells using a fluorescence-based binding assay. Chem. Biol. 19 (9), 1105–1115.
Tosh, D.K., Chinn, M., Ivanov, A.A., Klutz, A.M., Gao, Z.G., Jacobson, K.A., 2009. Functionalized congeners of A3 adenosine receptor-selective nucleosides containing a bicyclo[3.1.0]hexane ring system. J. Med. Chem. 52 (23), 7580–7592.
Trincavelli, M.L., Tuscano, D., Cecchetti, P., Falleni, A., Benzi, L., Klotz, K.N., Gremigni, V., Cattabeni, F., Lucacchini, A., Martini, C., 2000. Agonist-induced internalization and recycling of the human A3 adenosine receptors: role in receptor desensitization and resensitization. J. Neurochem. 75 (4), 1493–1501.
van der Putten, C., Zuiderwijk-Sick, E.A., van Straalen, L., de Geus, E.D., Boven, L.A., Kondova, I., Ijzerman, A.P., Bajramovic, J.J., 2009. Differential expression of adenosine A3 receptors controls adenosine A2A receptor-mediated inhibition of TLR responses in microglia. J. Immunol. 182 (12), 7603–7612.
Vernall, A.J., Hill, S.J., Kellam, B., 2014. The evolving small-molecule fluorescent-conjugate toolbox for class A GPCRs. Br. J. Pharmacol. 171 (5), 1073–1084.
Vernall, A.J., Stoddart, L.A., Briddon, S.J., Hill, S.J., Kellam, B., 2012. Highly potent and selective fluorescent antagonists of the human adenosine A(3) receptor based on the 1,2,4-Triazolo 4,3-a quinoxalin-1-one Scaffold. J. Med. Chem. 55 (4), 1771–1782.
Vernall, A.J., Stoddart, L.A., Briddon, S.J., Ng, H.W., Laughton, C.A., Doughty, S.W., Hill, S.J., Kellam, B., 2013. Conversion of a non-selective adenosine receptor antagonist into A3-selective high affinity fluorescent probes using peptide-based linkers. Org. Biomol. Chem. 11 (34), 5673–5682.
Verzijl, D., Ijzerman, A.P., 2011. Functional selectivity of adenosine receptor ligands. Purinergic Signal. 7 (2), 171–192.
Wan, T.C., Ge, Z.D., Tampo, A., Mio, Y., Bienengraeber, M.W., Tracey, W.R., Gross, G.J., Kwok, W.M., Achampach, J.A., 2008. The A3 adenosine receptor agonist CP-532,903 N-6-(2,5-dichlorobenzyl)-3'-aminoadenosine-5'-N-methylcarboxamide protects against myocardial ischemia/reperfusion injury via the sarcolemmal ATP-sensitive potassium channel. J. Pharmacol. Exp. Ther. 324 (1), 234–243.
Werthmann, R.C., Volpe, S., Lohse, M.J., Calebiro, D., 2012. Persistent cAMP signaling by internalized TSH receptors occurs in thyroid but not in HEK293 cells. FASEB J. 26 (5), 2043–2048.
Yaar, R., Lamperti, E.D., Toselli, P.A., Ravid, K., 2002. Activity of the A3 adenosine receptor gene promoter in transgenic mice: characterization of previously unidentified sites of expression. FEBS Lett. 532 (3), 267–272.
Yang, J.N., Chen, J.F., Fredholm, B.B., 2009. Physiological roles of A1 and A2A adenosine receptors in regulating heart rate, body temperature, and locomotion as revealed using knockout mice and caffeine. Am. J. Physiol. Heart Circ. Physiol. 296 (4), H1141–H1149.